27ème Colloque GRETSI sur le Traitement du Signal et des Images, Lille, France, 26-29 aout 2019.

Cultivons notre jardin avec Fourier

Salma SAMIEI, Pejman RASTI, François CHAPEAU-BLONDEAU, David ROUSSEAU
LARIS, UMR INRA IRHS, Université d'Angers, 62 avenue Notre Dame du Lac, 49000 Angers, France
surname.name@univ-angers.fr

Résumé – Dans cette communication nous exploitons l'imagerie de profondeur pour le suivi de la croissance de plantes. Nous montrons comment cette situation peut se ramener à un problème de traitement du signal. En plus du classique taux de croissance instantané, d'autres traits liés à la croissance apparaissent sous la forme de motifs répétitifs qui se prêtent à une analyse harmonique. Nous identifions l'origine de ces motifs et analysons comment ils peuvent être mis à profit dans des situations d'intérêt agronomique. Cette situation constitue une application originale de l'analyse de Fourier 197 ans après son introduction. Cet exemple, simple du point de vue de l'analyse, permet notamment en enseignement de sortir des cas classiques de signaux périodiques (sons, secteur électrique, ondes de diffusion, ...). Nous proposons à cet effet un exemple de jeu d'images et de données à analyser.

Abstract – In this report, we apply depth imaging to the monitoring of plants growth. We demonstrate that the situation can be understood as a signal processing problem. In addition to the instantaneous growth rate, other traits linked with growth appear under the form of periodic patterns that we analyze in the Fourier domain. We identify the cause of these periodic patterns and show their value for agronomic applications. This constitutes an original application of the Fourier analysis 197 years after its introduction. This simple example from a signal processing point of view is of high value in a teaching perspective if one seeks to provide illustrations that go beyond the classical domains for periodic signals (sounds, electrical voltage, heat, ...). We propose a data set as supplementary material to allow the reader to reproduce our analysis.

1 Introduction

Plant imaging is a topic of growing interest. In agronomy and biology, of course, plant imaging enables to automate and improve time-consuming measurements that used to be done manually. Also from the perspective of computer vision, plant imaging is now recognized as an applied field with its own specificities and challenges in a way similar to the bio-medical domain [1]. In this communication, we consider the problem of monitoring the growth of plants from top view. Depth imaging, which produces a distance map of an object in front of a camera to the camera, has been shown useful in such configurations to segment the upper leaves on individual plants[2]. This is especially interesting since in plants the color contrast is very low and that depth imaging is now available at low-cost (few hundred euros) through the use of "Kinect" like sensors. Here we consider the more complex situation where a population of plants possibly touching each other are positioned under a depth camera as visible in Fig. 1. Instead of developing algorithm to segment each individual plant we consider the 2.5D surface formed by the canopy of the plant as a whole. Under assumption of stationarity of the growth pattern from one plant to another we consider the average distance of this canopy to the camera as a signal characterizing the global growth of the population. This work proposes a signal processing analysis of the plant growth process. In comparison with the closest related work [3], we use very low-cost imaging systems (hundred euros versus keuros) while observing larger populations (hundred of plants versus ten plants), over a longer time scale including the appearance of new leaves (two weeks versus one week) and we demonstrate that this growth signal analysis can be used to recognize growth anomalies (while only controlled plants were exhibited in [3]). This is obtained with simple Fourier series while more advanced wavelet analysis were used in [3].

2 Image acquisition system

In this section, we briefly describe the imaging protocol used. We positioned a depth imaging system gazing from the top view on populations of plants automatically irrigated. The produced depth map is converted after sphericity correction into a distance map of the population of plants to the camera. The depth imaging system used is an active imaging system based on infrared lighting, it therefore enables to monitor plant growth during the night. The depth map are thresholded to remove the soil. The average value of this distance map is computed and plotted as a function of time with a time-lapse of one image every 15 minutes. Per depth image 100 plants are captured, which means that this imaging system has rather high throughput. The plants were observed during two weeks, after which they tend to bend and the distance to the camera no longer precisely corresponds to their actual height. Monitoring over these two weeks is however of great relevance since they correspond to the first two weeks of the plant life after emergence from the seed. This is a stage of interest for biologists since this is where photosynthesis is activated, and a stage of interest for breeders since this is the stage where they sale their products. This early stage is often crucial to the prognostic of the whole plant development and its yield. The plants monito-

red here were seedlings of sugar beet. However the approach can equally be applied to any species of interest.

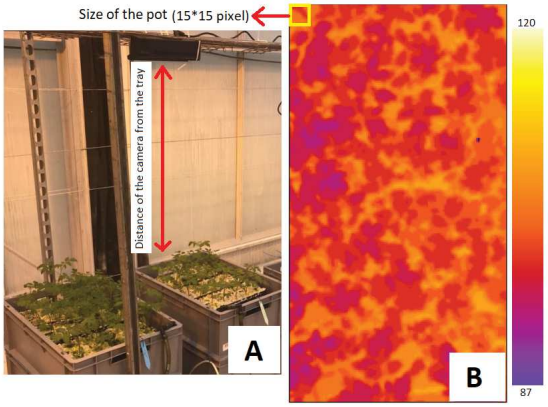

FIGURE 1 – Panel A, view of the image acquisition system. Panel B, colorized depth map with look up table "fire". The levels are indicated in cm.

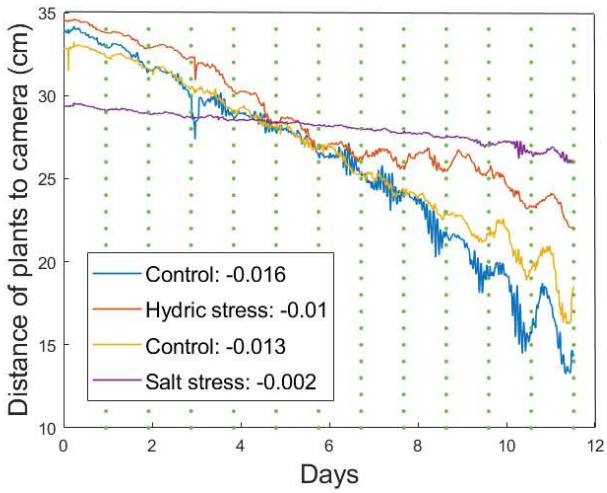

FIGURE 2 – Spatial average of the distance map $x(t)$ to the camera in cm as a function of time in various conditions. The values indicated in the inset correspond to average growth rates in centimeter per minute.

3 Qualitative signal analysis

Typical growth signals recorded with the imaging setup of the previous section are shown in Fig. 2. Different components are visible. First, a global linear trend shows the global growth of the plant which gets closer and closer to the camera. Second, some oscillations are visible at the exact day period. These oscillations correspond to the so-called circadian rhythm that allows plants (like most living organisms) to synchronize their physiology with the daily period of light, maximizing their ability to benefit from sunlight and minimizing energy loss when the light is not available [4]. A third component is visible and corresponds to a higher frequency pattern that occurs when leaves are replicated and produce some mechanical movements. For illustration, we propose in Fig. 2, an example of the growth curve for control plants and plants under stress (hydric or salt stress).

4 Design of a Fourier feature space

Before the introduction of low-cost depth imaging operating in the infrared domain, the monitoring of plant growth was somehow limited to the average growth rate. The monitoring of growth, as shown in Fig. 2, allows to quantify this process in more details. Following the qualitative description of the previous section, we propose to design a feature space based on a small set of numbers to encode the growth signal. The spatial average distance map to the camera $x(t)$ is first detrended with a daily linear trend which for the plants and growing duration selected in this study stands as a reasonable model. This produces the daily signal

$$y(t,n) = x(t) - (Gr(n) \times t + K) \tag{1}$$

with $t \in [nT, (n+1)T)]$ and

$$(Gr(n), K) = \text{argmin}_{\tilde{Gr},\tilde{b}} \sum_{t=nT}^{t=(n+1)T} (x(t) - (\tilde{Gr} \times t + \tilde{K}))^2 \tag{2}$$

where $Gr(n)$ simply measures the daily growth rate on day $n = \{0, 1, 2, ..., 12\}$ of the canopy and T is the daily period. Then, since the cellular processes can, from a theoretical biologic point of view [4], be assumed to be synchronized with the daily period of the sun, we decompose $y(t,n)$ as a Fourier series and compute the modulus of its fundamental

$$c_1(n) = \sqrt{a_1(n)^2 + b_1(n)^2} \tag{3}$$

with

$$a_1(n) = \frac{2}{T} \times \int_{nT}^{(n+1)T} y(t) \cos\left(\frac{2\pi}{T} t\right) dt \,, \tag{4}$$

$$b_1(n) = \frac{2}{T} \times \int_{nT}^{(n+1)T} y(t) \sin\left(\frac{2\pi}{T} t\right) dt \,. \tag{5}$$

The daily period T is assumed constant over the two weeks of observation. Energy in the daily sinus of amplitude $c_1(n)$ is found to represent more than 95% of $y(t,n)$ over the two weeks of observation. Therefore $c_1(n)$ constitutes a good approximation of the amplitude of the circadian cycles [3, 4]. However, to also capture the presence of the high frequency movements, we also consider the harmonic distortion rate

$$HDR(n) = 100 \times \sqrt{\frac{E(n) - \frac{1}{2} \times c_1(n)^2}{\frac{1}{2} \times c_1(n)^2}} \,, \tag{6}$$

where $E(n)$ is the energy of the detrended signal $y(t)$

$$E(n) = \frac{1}{T} \times \int_{nT}^{(n+1)T} y(t)^2 dt \,, \tag{7}$$

which captures the relative energy in the replication phenomenon of the leaves which causes the high frequency patterns. The instantaneous growth rate Gr obviously enables in Fig. 2 to differentiate between control plant and a stressed plant. However, when representing growth in a (HDR, c_1) graph, as in Figs. 3 and 4, with time as a parameter, it appears that these trajectories clearly differ also between control and stressed plants. Also, all recorded trajectories start with a low amplitude of the fundamental, then approximately after 6 days, an increase of the harmonic distortion rate with diminution of amplitude of fundamental follows, and after 10 days a decrease of the harmonic distortion rate and an increase of the fundamental. Trajectory learning could be undertaken in this feature space once we have more of these experiments. Here, we rather focus on the assessment of the added value of this extended feature space Gr, c_1, HDR when compared to the usual single scalar feature space based on the sole growth rate Gr. We propose a feature space which sums up the global shape of the temporal trajectories of Figs. 3 and 4 and consider the following 5-dimensional feature vectors

$$feat = (Gr, \max(c_1), \min(c_1), \max(HDR), \min(HDR)) \ . \tag{8}$$

We propose to compare the added value of this feature space when compared to the classical single growth rate Gr alone for two applications.

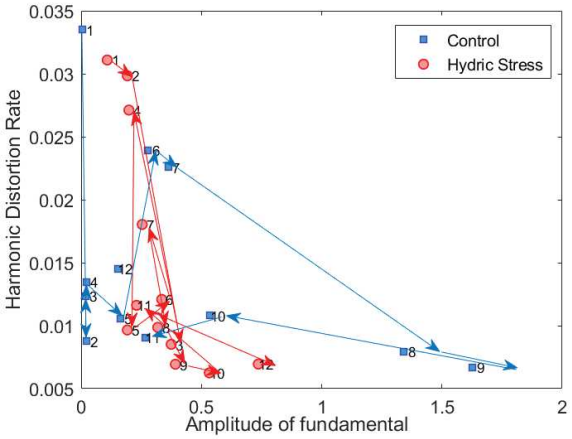

FIGURE 3 – Temporal trajectories of growth represented in a HDR, c_1 graph for control in blue and hydric stress in red. The arrows indicate the flow of time.

5 Applications

5.1 Best observation time

One of the biological questions that we can address with our feature space is, how to discriminate the plants which are in control condition from plants under stress. When is the best time to observe the differences between the plants in different situations ? To this purpose, we computed the Mean Square Error (MSE) of the feature vectors between control and stressed plants as a way of feature space contrast

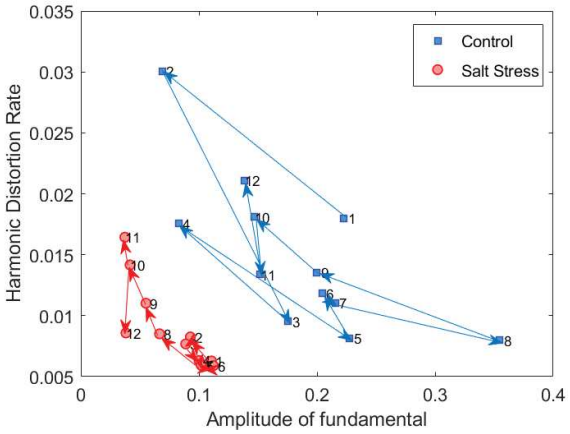

FIGURE 4 – Same as in Fig. 3 but with red for salt stress.

$$MSE = \frac{1}{5}\sum_{i=1}^{5}(feat_c(i) - feat_s(i))^2, \tag{9}$$

where $feat_c$ is the feature vector for the control and $feat_s$ for the stressed plant. As shown in Figs. 5 and 6, the extended feature space based on $feat$ of Eq. (8) can be above the basic reference of the growth rate at early stages, but it is difficult to have a definite point on this since only two records were done. However, it seems obvious from Figs. 5 and 6 and from Fig. 2 that the contrast (MSE) between stressed plant and control plant is much higher after ten days with the extended feature space proposed here and the usual single growth rate. This is the best observation time if one wants to take benefit from the extended feature space based on Fourier analysis proposed here.

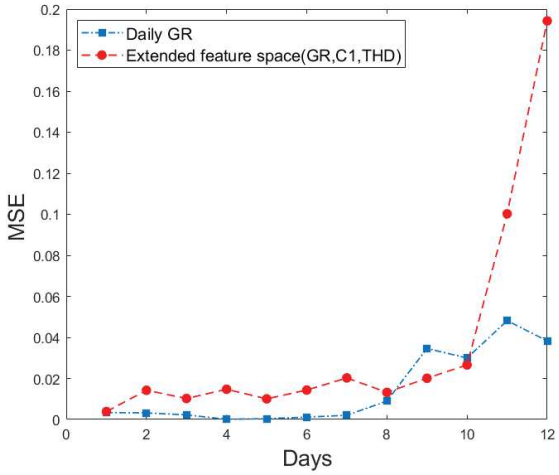

FIGURE 5 – Contrast between control and salt stress for the sole growth rate (Daily GR) and for the extended feature space of Eq. (8) computed by the MSE of Eq. (9).

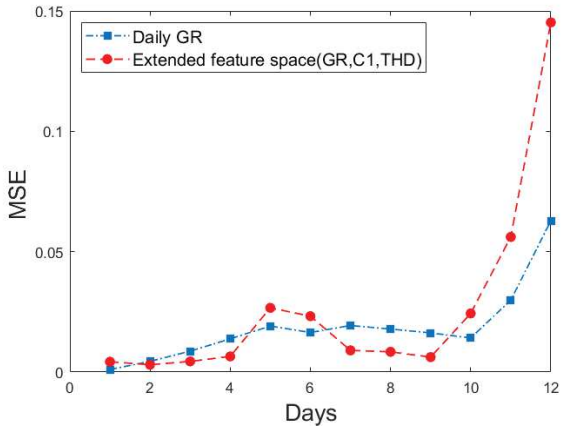

FIGURE 6 – Same as in Fig. 5 but with hydric stress.

5.2 Stress detection

To further assess the interest of the proposed extended feature space of Eq. (8) we go beyond contrast metric and implement a supervised detection scheme to classify stressed plants from a control plants. The feature extracted from Eq. (8) are fed to a support vector machine (SVM) with linear kernel. The effectiveness of SVM classifier is evaluated by the K-fold cross-validation K=10. [5]. For comparison the sole growth rate is computed and applied to the same support vector machine classifier. Small images of size 15 by 15 pixels are created in depth maps as shown in Fig. 1. This corresponds to the size of a single pot. The performance of the classification is given in terms of accuracy based on the following formula

$$accuracy = \frac{TP + TN}{Total} \ , \qquad (10)$$

where TP stands for the true positive and TN for the true negative. The accuracies for classifications based on the extended feature space of Eq. (8) and the sole growth rates are given in Table 1. This clearly demonstrates a gain between 4% and 9% of accuracy when the feature space is extended to the Fourier-based features of Eq. (8). Measuring the amplitude of the circadian cycle and the distortion rate of these circadian cycles improves efficiency to discriminate control from stressed plants.

6 Conclusion

197 years after the introduction of the Fourier analysis [6], its ubiquitous applicability was again illustrated in this communication with recent low-cost imaging systems to monitor the growth of plants. In this context we designed a feature space based on Fourier analysis and demonstrated its interest on agronomical applications. Accumulated data will enable in the future more applications in the direction of deeper understanding of the temporal trajectory of growth in this feature space. So far the material produced here can already be used for educational purposes to provide the students with new application fields of the Fourier analysis. To this purpose we give access to raw data of our experiment in `https://uabox.univ-angers.fr/index.php/s/hf2csYRguVKNtWy`.

	Accuracy K-fold K=10
GR FS Control, Hydric Stress	83.1%
GR FS Control, Salt Stress	94.8%
Extended FS Control, Hydric Stress	92.2%
Extended FS Control, Salt Stress	99%

TABLE 1 – Accuracy for the SVM K-fold (K=10) cross-validation classification between stressed plants from control plants with a feature space only based on growth rate (GR FS) or based on our extended feature space of Eq. (8) (Extended FS).

7 Acknowledgement

This work received support from the french government supervised by the Agence Nationale de la Recherche in the framework of the program Investissements d'Avenir under reference ANR-11-BTBR-0007 (AKER program) and Labcom ESTIM.

Références

[1] Minervini Massimo, Scharr Hanno and Tsaftaris, Sotirios A, "Image analysis : the new bottleneck in plant phenotyping" *IEEE Signal Processing Magazine*, vol. 32, pp 126–131, 2015.

[2] Chéné Yann, Rousseau David, Lucidarme Philippe, Bertheloot Jessica, Caffier, Valérie, Morel Philippe, Belin Étienne, Chapeau-Blondeau François, "On the use of depth camera for 3D phenotyping of entire plants", *Computers and Electronics in Agriculture*, vol. 82, pp 122–127, 2012.

[3] Bours, Ralph and Muthuraman, Manickam and Bouwmeester, Harro and van der Krol, Alexander, "OSCILLATOR : a System for Analysis of Diurnal Leaf Growth using Infrared Photography Combined with Wavelet Transformation", *Plant Methods*, vol. 8, pp. 1–29 2012,

[4] McClung, C Robertson, "Plant Circadian Rhythms" *The Plant Cell*, vol. 18, pp 792–803, 2006.

[5] Cornuéjols, Antoine et Miclet, Laurent, "Apprentissage artificiel : concepts et algorithmes", Eyrolles, 2011.

[6] Fourier, Joseph, "Théorie Analytique de la Chaleur", Firmin Didot, père et fils, 1822.